JACS
JOURNAL OF THE AMERICAN CHEMICAL SOCIETY
Communication
pubs.acs.org/JACS

Significant Hydration Shell Formation Instead of Hydrogen Bonds in Nanoconfined Aqueous Electrolyte Solutions

Tomonori Ohba,*[,†] Kenji Hata,[‡] and Hirofumi Kanoh[†]

[†]Graduate School of Science, Chiba University, 1-33 Yayoi, Inage, Chiba 263-8522, Japan

[‡]Nanotube Research Center, National Institute of Advanced Industrial Science and Technology (AIST), 1-1-1 Higashi Tsukuba, Ibaraki 305-8565, Japan

Supporting Information

ABSTRACT: Nanoscale confined electrolyte solutions are frequently observed, specifically in electrochemistry and biochemistry. However, the mechanism and structure of such electrolyte solutions are not well understood. We investigated the structure of aqueous electrolyte solutions in the internal nanospaces of single-walled carbon nanotubes, using synchrotron X-ray diffraction. The intermolecular distance between the water molecules in the electrolyte solution was increased because of anomalously strong hydration shell formation. Water correlation was further weakened at second-neighbor or longer distances. The anomalous hydrogen-bonding structure improves our understanding of electrolyte solutions in nanoenvironments.

Nanoscale confined aqueous electrolyte solutions play an essential role in chemical and biological processes, for example, in electrochemical capacitors and ion channels. Batteries and electric double-layer capacitors have attracted attention recently for environmentally friendly electric power sources.[1] Electric double-layer capacitors are expected to have high power and energy densities, which would compensate for the disadvantages of batteries and conventional capacitors. Nanoporous carbons, such as activated carbon, carbide-derived carbon, and carbon nanotubes (CNTs), have been used as electrodes, because of their high surface area and conductivity and electrochemical stability.[2] Electrolytes can enter and exit the nanospaces in such electrodes during the charge and discharge cycles in electric double-layer capacitors. It is therefore desirable to investigate the mechanism and structure of electrolyte solutions in nanospaces, to allow the development of efficient storage devices for electric double-layer capacitors. Gogotsi and Simon reported the dependence of the capacitance on the nanospace size.[3] The removal of the solvation shell of ions, and the mobility of the ions, significantly affected their capacitance efficiency. However, the details of the structure of electrolyte solutions, the hydration shell formation, and the dehydration in the nanospaces remain poorly understood. In the case of ion channels, various ion channels in biomembranes have nanospaces as well as gates for selective separation of ions; these structures allow the selective penetration of target ions into their nanospaces.[4] In this manner, ion channels transmit and receive electrical signals by controlling the flow of ions and fluid. Thus, the mechanism of ions in ion channels is the key to understanding the biological activity. However, gaining an understanding of the mechanism by which ions penetrate the nanospaces of ion channels is made difficult by the complexity and flexibility of the nanospaces. Thus, a simple and rigid nanospace model is required to advance our understanding of this process.

CNTs are a simple idealized model system for the investigation of the behavior of electrolyte solutions in nanospaces, because CNTs are composed of only carbon atoms and have simple one-dimensional nanospaces.[5] Some studies have investigated the mechanism of electrolyte solutions in nanospaces, using CNTs and related porous carbons to elucidate the behavior of the electrolyte solutions, mainly via molecular dynamics (MD) simulations; energy barriers to ion penetration through hydrophobic nanospaces, and the dehydration of ions in narrow hydrophobic nanospaces were observed in MD and Monte Carlo simulations.[6] MD simulations have also shown that ion separation should be possible using CNTs;[7] other studies on the behavior of electrolyte solutions in CNTs evaluated the transportation properties of ions in hydrophobic nanospaces.[8] Ohkubo and co-workers evaluated the hydration numbers of ions in hydrophobic nanospaces experimentally, using extended X-ray absorption fine structure analysis.[9] Significant dehydration of ions in the nanospaces was observed, agreeing with our simulation studies.[6b] Levi and co-workers evaluated the solvation numbers of alkalis, alkaline earth cations, and halogen anions in carbon nanospaces and observed significant desolvation.[10] However, the hydration shell structure in aqueous electrolyte solutions is far from understood, despite the fact that several MD simulations and some experimental studies have been performed. To the authors' knowledge, experimental studies on the hydration structure in electrolyte solution systems have rarely been performed. In this communication, we determine the hydration shell structure via an electron radial distribution analysis of the synchrotron X-ray diffraction (XRD) patterns for aqueous electrolyte solutions in CNTs.

Here, the CNTs were synthesized using the supergrowth method reported by Hata and co-workers.[11] The CNTs were single-walled, without metal impurities, and had internal nanospaces with an average diameter of 2 nm.[12] CNTs of relatively large diameter were used, because they allowed the electrolyte solutions in the CNTs to be observed more easily. It

Received: July 26, 2012
Published: October 22, 2012

dx.doi.org/10.1021/ja307338t | J. Am. Chem. Soc. 2012, 134, 17850−17853

should be noted that the average diameter of the CNTs was rather larger than that of an ion channel in a cell, whose narrowest point is approximately 0.3−0.5 nm in diameter. The CNTs rarely aggregated, although some CNT bundles were observed. The external surfaces of the CNTs were hydrophobic and thus had a shallow adsorption potential for water and aqueous electrolyte solutions. However, the interstitial nanospaces between the CNTs, which had a strong adsorption potential, were smaller in volume than the internal CNT spaces. Therefore, water was adsorbed mainly in the internal CNT spaces. After evacuating the samples at approximately 1 Pa for 2 h and at 303 K, the CNTs were immersed in a 1 mol L^{-1} NaCl aqueous solution, or water, for 5 days, to allow the system to completely reach equilibrium. The CNTs were then removed from those solutions, and the external surfaces of CNTs were promptly washed using deionized water. The CNTs were quickly placed in an XRD capillary tube, and the relative humidity was controlled at 80−90% for 2 days, so that the water content could be maintained in the internal CNT spaces but not on the external surfaces, as mentioned above. Here, the 1 mol L^{-1} NaCl aqueous solution and the water in the internal CNTs nanospaces are respectively named 'nanoelectrolyte' and 'nanowater'. XRD measurements on the nanoelectrolyte and nanowater in the CNTs were performed at SPring-8, at a wavelength λ of 0.1000 nm and 303 K; XRD measurements were also performed on CNTs in vacuo, a bulk NaCl aqueous solution, and bulk water, for comparison. The accumulation time was 0.5 h for all of the samples described above. The electron radial distribution functions (ERDFs) for the nanoelectrolyte and nanowater were obtained from Fourier transforms of the XRD patterns calculated by subtracting the patterns for the nanoelectrolyte and nanowater in CNTs from the pattern for CNTs in vacuo. The ERDFs for the bulk electrolyte solution and water were also obtained to allow a comparison.

The CNTs used in this study were single-walled and had internal nanospaces with an average diameter of 2 nm; these dimensions were evaluated from transmission electron microscopy images, and an N_2 adsorption isotherm measured at 77 K (see Supporting Information, SI, and previous studies).[12] The nanospace volume in the CNTs was evaluated as 0.69 mL g^{-1}, from an α_S analysis of the N_2 adsorption isotherm. The water vapor adsorption isotherm for CNTs at 303 K (shown in Figure S1) indicates that ∼0.69 g of water could be adsorbed on 1 g of CNTs, i.e., there was 0.69 g of water per 1 g of carbon in the CNTs. The sum of the atomic scattering intensities for the adsorbed water was 1.3 times larger than that for the CNTs. This was determined using the above relation, with atomic scattering intensities of 66 for water and 36 for carbon. Here, the scattering intensity for the ions was increased by 5% of the total intensity, under the assumption of the scattering intensity ratio $Na^+:Cl^-:H_2O:C$ = 0.07:0.22:2.53:3.00 (details in SI). XRD patterns are shown in Figure 1 for the nanoelectrolyte and nanowater. Here, the scattering parameter is defined by $s = 4\pi \sin\theta / \lambda$. The XRD pattern for CNTs in vacuo is given to allow a comparison with the nanoelectrolyte and nanowater. The XRD intensities were adjusted using the above-mentioned relation for the atomic scattering intensities. Significant small-angle X-ray scattering was observed for all samples. For the CNTs, the largest small-angle X-ray scattering intensity was observed below 12 nm^{-1}. The smaller intensities observed for the nanoelectrolyte and nanowater in these regions (compared with that observed for the CNTs) are the result of adequate filling with nanoelectrolyte and nanowater in the internal CNT nanospaces. In addition, the small-angle X-ray scattering from the nanoelectrolyte was slightly smaller than that from the nanowater, indicating the uniform water structures in the CNTs. In contrast, the nanowater formed cluster-like structures, as mentioned in previous literature.[13,14] The XRD pattern for the CNTs shows three different XRD peaks at 15, 28, and 49 nm^{-1}, indicating lattice distances of 0.42, 0.22, and 0.12 nm, respectively. The first peak was assigned to the spacing between the graphene layers of adjacent CNTs. The second and third peaks were due to graphene intralayer reflections. In the case of the nanoelectrolyte and nanowater, significant scattering was observed in the s range of 12−30 nm^{-1}. The large scattering intensities were due to the presence of nanoelectrolyte or nanowater; this was confirmed by the significant scattering observed in the bulk electrolyte solution and bulk water in the range of 10−30 nm^{-1}, as shown in Figure S2. The scattering at approximately 20 nm^{-1} was caused by intermolecular scattering from adjacent water.

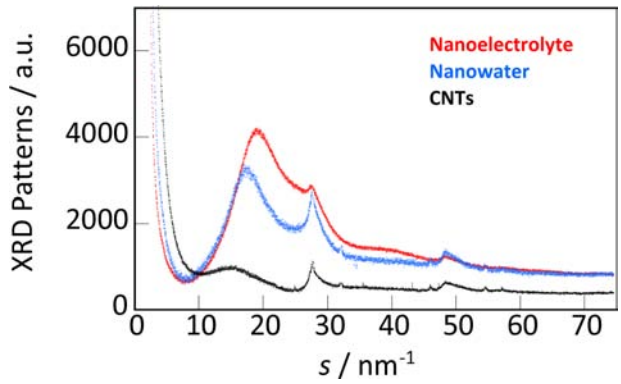

Figure 1. XRD patterns for CNTs with electrolyte solution or water in the internal CNT nanospaces and CNTs in vacuo. The electrolyte solution was a 1 mol L^{-1} NaCl aqueous solution that filled the CNTs.

The differences between the scattering from the nanoelectrolyte or nanowater and that from the CNTs highlighted the scattering from the aqueous electrolyte solution or water confined in the nanospaces, respectively (see Figure S3). The shape of the nanoelectrolyte and nanowater was apparently different from those of the bulk electrolyte solution and bulk water, as shown in Figure S2. However, the scattering pattern for the bulk electrolyte solution was quite similar to that for the bulk water, and the peak positions were at approximately 20, 30, and 40−50 nm^{-1}. This indicates that the intermolecular scattering between water itself is dominant, i.e., ions rarely influence the whole structure of the bulk electrolyte solution. The scattering from the nanoelectrolyte was different from that from the nanowater, in spite of the similarities between the scattering from the bulk electrolyte solution and the bulk water. In the range of 20−40 nm^{-1}, the peaks were more intense and broader for the nanoelectrolyte than for the nanowater. The first peak for nanowater was sharper than that for the bulk, whereas that for the nanoelectrolyte was broader. This suggests that the water structure in the nanoelectrolyte is flexible, in contrast with that in the nanowater.

The ERDFs were obtained from the differential XRD profiles, as shown in Figure 2 (see peak position in Table S1). The ERDFs for the bulk electrolyte solution and bulk water were similar to each other, as expected from the XRD

dx.doi.org/10.1021/ja307338t | J. Am. Chem. Soc. 2012, 134, 17850−17853

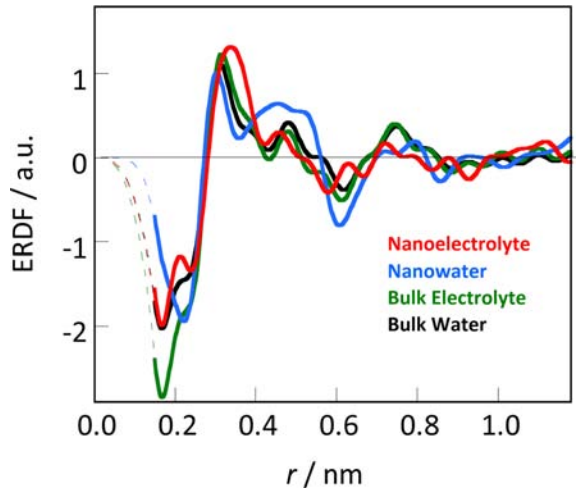

Figure 2. ERDFs for nanoelectrolyte solution, nanowater, bulk electrolyte solution, and bulk water. Distances smaller than 0.14 nm were disregarded for all fluids.

patterns. The nearest-neighbor distance between molecules, i.e., the intermolecular distance, was 0.31 nm for the bulk electrolyte solution and bulk water, and relatively weak second- and third-neighbor distributions were also observed at approximately 0.5 and 0.7 nm, which were assigned to the second- and third-neighbor distances of water. The intermolecular distance was 0.30 nm for nanowater, and a significant distribution was observed at 0.40−0.53 nm. The third-neighbor peak at 0.72−0.80 nm was more weakly observed than in the bulk water. This is a result of nanoscale ice formation, as described in a previous paper.[13] These results show that a strong hydrogen-bonding water network was formed in the nanowater. In the case of the nanoelectrolyte, the nearest-neighbor peak was broad and centered at 0.34 nm. Thus, the intermolecular distance was 0.03 nm longer than that in the bulk electrolyte solution. The first peak, i.e., the first-neighbor distance in the nanoelectrolyte, can be assigned to the intermolecular distances between water−water, Na^+−water, and Cl^-−water. Here, the scattering intensities from Na^+ and Cl^- respectively represented 2% and 8% of the total scattering evaluated from the above-mentioned ratio. Thus, the intermolecular distance between Na^+−Cl^- could not be observed because of the extremely small scattering intensities. The distances for Na^+−water and Cl^-−water were expected to be 0.23 and 0.34 nm, respectively.[15] Hence, the broad peak at 0.34 nm is attributed to not only water−water but also Cl^-−water. On the other hand, the effective structure assigned to Na^+−water could not be observed, because the peak at 0.21 nm was also observed for the bulk water. The second and third peaks were roughly similar to those observed for the bulk electrolyte solution and bulk water, although the peak positions were similar to those observed for nanowater, rather than the bulk electrolyte solution and bulk water. The significant peaks for the second- and third-neighbor distances in the nanoelectrolyte therefore nearly disappeared. These results indicate that the hydrogen bonds of the water are stretched and broken at longer distances. This is a result of the predominant hydration shell formation of ions, instead of the hydrogen-bonding formation of water. Therefore, the formation of the first hydration shell was significantly enhanced by the interaction of water with ions in the nanospaces. On the other hand, the long-range correlation between the water was weakened for distances longer than 0.4 nm.

In this communication, the structure of nanoelectrolytes was elucidated via a synchrotron XRD analysis of aqueous electrolyte solutions in CNTs. The intermolecular distance of water in the nanoelectrolyte was stretched, and the hydrogen bonds between water molecules were simultaneously weakened, whereas in the nanowater, nanoscale assembled structure formation was observed with strong hydrogen bonding. This was the result of the anomalously enhanced hydration shell formation by the ions in the nanoelectrolyte. The water structure of the hydration shells in nanoelectrolytes was experimentally revealed for the first time and was shown to be efficient for building a model of electrolyte solutions in nanospaces and at nanointerfaces. This work clarifies the mechanism of aqueous electrolyte solutions in nanospaces, although the hydration numbers and detailed hydration structures are as yet unknown. These details could be revealed by molecular simulations and associated experimental work. Further studies on the temperature effect and the dependence of pore size and geometry are also necessary to understand aqueous electrolyte solutions in nanospaces in more detail.

■ ASSOCIATED CONTENT

Supporting Information

N_2 adsorption isotherm at 77 K and water vapor adsorption isotherm at 303 K for CNTs, XRD patterns for bulk electrolyte solution and water, differential XRD patterns for nanoelectrolyte and nanowater, and peak positions of ERDFs. This material is available free of charge via the Internet at http://pubs.acs.org.

■ AUTHOR INFORMATION

Corresponding Author

ohba@pchem2.s.chiba-u.ac.jp

Notes

The authors declare no competing financial interest.

■ ACKNOWLEDGMENTS

We thank Dr. J. Kim and Dr. N. Tsuji for their help in recording the XRD data at SPring-8. This research was supported by a Research Fellowship from the Foundation for the JGC-S Scholarship Foundation, Promotion of Ion Engineering, Murata Science Foundation, Nippon Sheet Glass Foundation, and Global COE Program, Japan.

■ REFERENCES

(1) (a) Simon, P.; Gogotsi, Y. *Nat. Mater.* **2008**, *7*, 845−854. (b) Huang, J.; Sumpter, B. G.; Meunier, V. *Chem.—Eur. J.* **2008**, *14*, 6614−6626. (c) Frackowiak, E.; Beguin, F. *Carbon* **2002**, *40*, 1775−1787.

(2) (a) Yoon, B. −J.; Jeong, S. −H.; Lee, K. −H.; Kim, H. S.; Park, C. G.; Han, J. H. *Chem. Phys. Lett.* **2004**, *388*, 170−174. (b) Zhai, Y.; Dou, Y.; Zhao, D.; Fulvio, P. F.; Mayes, R. T.; Dai, S. *Adv. Mater.* **2011**, *23*, 4828−4850.

(3) (a) Chmiola, J.; Yushin, G.; Gogotsi, Y.; Portet, C.; Simon, P.; Taberna, P. L. *Science* **2006**, *313*, 1760−1763. (b) Simon, P.; Gogotsi, Y. *Acc. Chem. Res.* DOI: 10.1021/ar200306b. (c) Chmiola, J.; Largeot, C.; Taberna, P. L.; Simon, P.; Gogotsi, Y. *Angew. Chem., Int. Ed.* **2008**, *47*, 3392−3395.

(4) (a) Mackinnon, R. *Angew. Chem., Int. Ed.* **2004**, *43*, 4265−4277. (b) Collins, K. D.; Neilson, G. W.; Enderby, J. E. *Biophys. Chem.* **2007**, *128*, 95−104.

(5) Sansom, M. S. P.; Biggin, P. C. *Nature* **2001**, *414*, 156−157.

(6) (a) Beckstein, O.; Tai, K.; Sansom, M. S. P. *J. Am. Chem. Soc.* **2004**, *126*, 14694−14695. (b) Ohba, T.; Kojima, N.; Kanoh, H.; Kaneko, K. *J. Phys. Chem. C.* **2009**, *113*, 12622−12624.
(7) (a) Park, J. H.; Sinnott, S. B.; Aluru, N. R. *Nanotechnology* **2006**, *17*, 895−900. (b) Liu, H.; Jameson, C. J.; Murad, S. *Mol. Sim.* **2008**, *34*, 169−175. (c) Gong, X.; Li, J.; Xu, K.; Wang, J.; Yang, H. *J. Am. Chem. Soc.* **2010**, *132*, 1873−1877.
(8) (a) Hummer, G.; Rasaiah, J. C.; Noworyta, J. P. *Nature* **2001**, *414*, 188−190. (b) Berezhkovskii, A.; Hummer, G. *Phys. Rev. Lett.* **2002**, *89*, 064503. (c) Shao, Q.; Zhou, J.; Lu, L.; Lu, X.; Zhu, Y.; Jiang, S. *Nano Lett.* **2009**, *9*, 989−994. (d) Shao, Q.; Huang, L.; Zhou, J.; Lu, L.; Zhang, L.; Lu, X.; Jiang, S.; Gubbins, K. E.; Shen, W. *Phys. Chem. Chem. Phys.* **2008**, *10*, 1896−1906.
(9) (a) Ohkubo, T.; Takehara, Y.; Kuroda, Y. *Microporous Mesoporous Mater.* **2012**, *154*, 82−86. (b) Ohkubo, T.; Konishi, T.; Hattori, Y.; Kanoh, H.; Fujikawa, T.; Kaneko, K. *J. Am. Chem. Soc.* **2002**, *124*, 11860−11861.
(10) Levi, M. D.; Sigalov, S.; Salitra, G.; Elazari, R.; Aurbach, D. *J.Phys. Chem. Lett.* **2011**, *2*, 120−124.
(11) Hata, K.; Futaba, D. N.; Mizuno, K.; Namai, T.; Yumura, M.; Iijima, S. *Science* **2004**, *306*, 1362−1364.
(12) Ohba, T.; Matsumura, T.; Hata, K.; Yumura, M.; Iijima, S.; Kanoh, H.; Kaneko, K. *J. Phys. Chem. C* **2007**, *111*, 15660−15663.
(13) Ohba, T.; Taira, S.; Hata, K.; Kaneko, K.; Kanoh, H. *RSC Adv.* **2012**, *2*, 3634−3637.
(14) (a) Ohba, T.; Kanoh, H.; Kaneko, K. *Nano Lett.* **2005**, *5*, 227−230. (b) Ohba, T.; Kanoh, H.; Kaneko, K. *J. Phys. Chem. C* **2012**, *116*, 12339−12345.
(15) Liu, Y.; Ichiye, T. *J. Phys. Chem.* **1996**, *100*, 2723−2730.